Extended Visual Servoing

Hong Zhang
College of Engineering
Rowan University, Glassboro, NJ 08028
zhang@galaxy.eng.rowan.edu

Noah John Cowan
Department of Integrative Biology
University of California, Berkeley CA 94720
ncowan@socrates.berkeley.edu

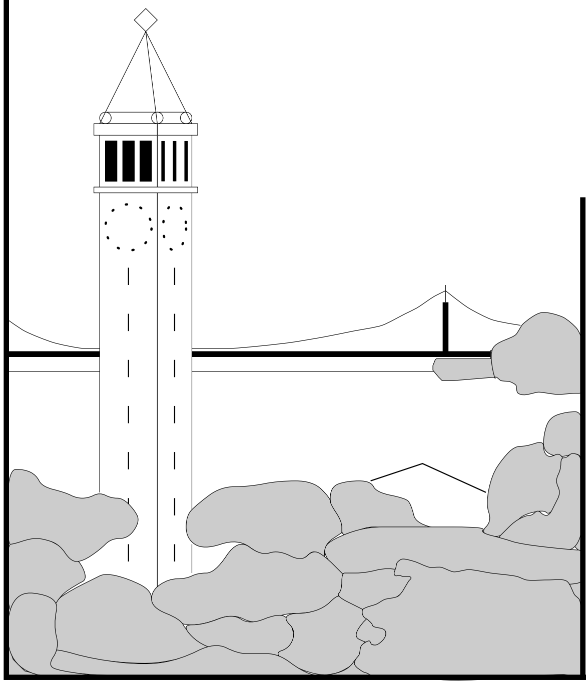

Report No. UCB/CSD-03-1237

April, 2003

Computer Science Division (EECS)
University of California
Berkeley, California 94720

Abstract

We present initial progress on so-called *extended visual servoing*, an integrated approach of controlling mobile robots equipped with multiple sensors. Our approach to sensor fusion uses the mathematical framework of visual servoing for a higher dimensional feature space that incorporates other sensors in addition to vision (which still plays a central role). Analysis and simulation on a planar mobile robot with "vision + sonar" shows the initial success of the approach.

1 Introduction

This technical report builds on visual servoing, which takes advantage of the rapid advancement of camera and image processing technologies in order to provide feedback information for a robot controller [7, 8]. There are two approaches to visual servoing: position-based and image-based. Position-based methods use a geometric model of the target to estimates the position and orientation of the body being servoed, and then compute the control inputs in Cartesian coordinates [13]. Image-based visual servoing computes the control inputs directly from the image features [7], and it is thought to be more robust with respect to camera calibration uncertainty. Image-based approaches generally require the so-called image Jacobian, the computation of which usually requires the depth of features being tracked [8]. Different methods address this drawback, such as 2-1/2D visual servoing [10], stereo [9], or the use of a calibrated target [4, 15]. However, they all introduce certain challenges, such as extra landmark points for 2-1/2D visual servoing, expensive hardware and extra computation for stereo vision, or restriction to a limited selection of special landmarks.

Most visual servoing methods have been developed for robot arms, but may be simply transfered to the control of a mobile robot. In addition to vision, however, most mobile robot platforms are equipped with extra motion sensors in addition to vision, such as sonar [11, 14], laser range finders, compasses, etc. Sensor fusion algorithms generally focus on object pose estimation [1, 2], rather than control. Therefore, we present a new approach to robot control by directly applying feedback from multiple sensors.

Our method is built on ideas of image-based visual servoing. The goal of visual servoing is to move the robot to a position and orientation such that the view of a scene obtained from a camera will match a predefined one that is stored in memory. This report takes the natural next step to broaden our notion of the "view" to include sensor values from multiple sensors, rather than just vision. Due to its versatility, vision still take a central role, so we call the approach ***Extended Visual Servoing***. Our approach inherits several useful features from image-based visual servoing:

- *Computational simplicity.* There is no need to transform sensor features to configuration space as position-based visual servoing and most sensor fusion methods.

- *Independent of object model.* The precise geometric property of the object is not necessary since the control is based on the sensor features only.

- *Robustness to sensor and robot calibration uncertainty.* The feedback loop is closed around sensor readings, decreasing sensitivity to sensor and robot calibration.

By incorporating several sensor modalities, it may be possible to take advantage of each sensor's relative strengths to complement the weaknesses of others. Sonar applications, for example, are usually restricted to obstacle detection and avoidance (rather than tracking) since it is challenging to use sonar to distinguishing between specific features. Vision systems, by contrast, provide a means by which to distinguish between features, but are poor feature depth estimators. This is a critical shortfall for visual servoing because the image Jacobian almost invariably depends on the depths of the features being viewed. Hence, we argue, sonar is an ideal complementary sensor to augment a monocular visual servoing system. Thus, we exploit the synergy between vision and sonar, by taking advantage the strengths of both sensors to control a robot.

This paper is arranged as following. After the introduction in this section, we will model sensors and their features in Section 2, then officially introduce the idea of extended visual servoing in Section 3. An example of applying the techniques with camera and sonar on a planar mobile robot will be given in Section 4. In last section, we will give some summaries and remarks.

2 Feature Space

For a 2D ground mobile robot, the perspective projection of an object will bring us one measurable variable γ in the image plane. Thus, the ***image feature space*** considered in this paper is the simple projection of a single point feature onto a 2D image plane, as described below. In addition to the camera, we assume that a sonar system augments the vision system to provide an ***extended feature space***, as described below.

2.1 Camera Feature

For simplicity, we employ a simple, calibrated 2D pinhole camera with perspective projection (Fig. 1).

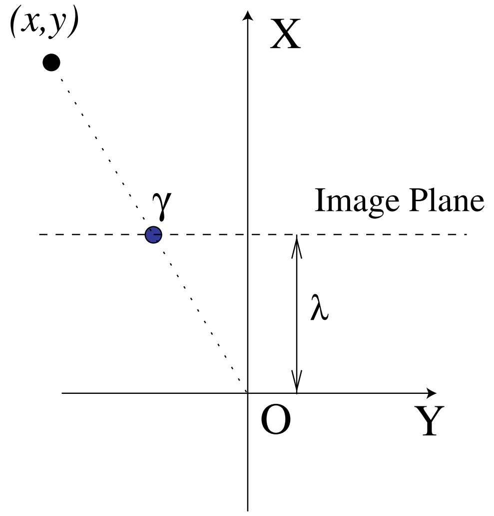

Figure 1: Perspective projection for a planar pinhole camera.

As shown in Fig. 1, the origin of the *camera frame* is given by O. The X-axis is the optical axis that is perpendicular to the image plane and points forward from the lens.[1] Let $p = [x, y]^T$ be the position of a point in camera frame. Then γ is its ***projection*** on the image plane, given by

$$\gamma = \lambda \frac{y}{x}. \tag{1}$$

where λ is the ***focal length***.

[1] The choice of axes labels is slightly different from the common choice in the literature.

2.2 Sonar Feature

Though there are many sensor suites from which to choose, we model our sonar system as sequentially triggered, narrow beam transducer that can measure distance from reflective surfaces, as shown in Fig. 2. The sonar sensors are configured as an equally distributed ring (only one sonar, at location β, is explicitly illustrated in the figure). The sensitive area of the sensor is shown as an angle ϕ, which is generally less than 25° for a narrow beam sonar.

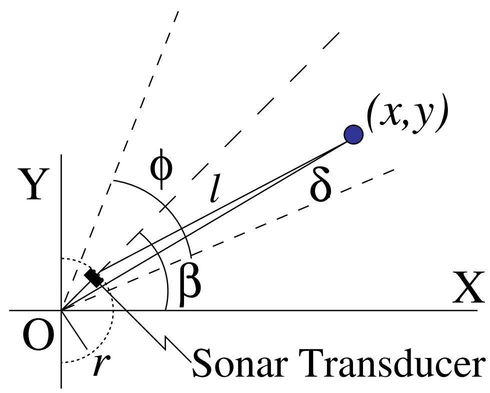

Figure 2: Reflective model of a narrow beam sonar.

The specular surface of the object in field will bounce the sound wave back to the original transducer, to measure the distance from the sensor to the object,

$$l = c \cdot t_{\mathrm{TOF}}/2, \tag{2}$$

where c is the speed of sound in air and t_{TOF} is the "time of flight" of the echo, i.e. the time duration from the instant the sonar is activated to the moment the echo is received. If the radius of the sonar ring is r, the distance from an object located at (x, y) with respect to the sonar center O can be approximated as

$$\delta = l + r = (x^2 + y^2)^{\frac{1}{2}} \tag{3}$$

as long as $l \geq r$. The angle of the target is often approximated as the angle of the sonar β, but the error is too large to be feasible in this paper.

2.3 Combining Vision and Sonar

We define the overall sensor information that can be acquired for a robot regarding its motion as the ***senso-***

rium, $\mathcal{S}$. In the simple example presented in this section, $\mathcal{S} = \mathbb{R} \times \mathbb{R}^+$, since the image plane is represented by $\gamma \in \mathbb{R}$ and the sonar measurement is represented by $\delta > 0$. Further, we categorize all the corresponding properties of the environment being measured by sensors as ***landmarks***, $\mathcal{L}$. Again, in the simple example in this section, there is a single landmark, which is a point in the planar world, so $\mathcal{L} = \mathbb{R}^2$. Therefore, we model the sensor suite as a mapping from the landmarks to sensorium, $h : \mathcal{L} \to \mathcal{S}$. In our case, assuming the camera and sonar frames are collocated for convenience, we have

$$h(p) = \begin{bmatrix} \lambda x/y \\ \sqrt{x^2 + y^2} \end{bmatrix}, \quad \text{where} \quad p = \begin{bmatrix} x \\ y \end{bmatrix}. \tag{4}$$

3 Extended Visual Servoing

In this section, we present a general approach to extended visual servoing that we will restrict later to the case of a planar, unicycle-type mobile robot.

3.1 Rigid Kinematics

We consider the problem of positioning a robot using feedback from onboard sensors. The configuration space of a mobile robot is modeled as $\mathcal{G} = \mathrm{SE}(3)$ for a spacial robot or $\mathcal{G} = \mathrm{SE}(2)$ for a planar robot. Therefore, the pose of the robot is given by a rigid transformation matrix

$$g = \begin{bmatrix} R & d \\ 0^T & 1 \end{bmatrix} \in \mathcal{G}$$

where d and R are the position and orientation of the robot expressed in the fixed world frame, respectively. Recall that $T\mathcal{G} \simeq \mathcal{G} \times \mathfrak{g} \simeq \mathcal{G} \times (\mathbb{R}^{n(n-1)/2} \circledS \mathbb{R}^n)$, where $\mathfrak{g} = T_I\mathcal{G}$ is the tangent space at the identity [12]. We make the identification via the "left inverse", namely if $(g, \dot{g}) \in T\mathcal{G}$, then, for $\mathcal{G} = \mathrm{SE}(3)$, we have

$$\xi = g^{-1}\dot{g} = \begin{bmatrix} 0 & -\omega_z & \omega_y & v_x \\ \omega_z & 0 & -\omega_x & v_y \\ -\omega_y & \omega_x & 0 & v_z \\ 0 & 0 & 0 & 0 \end{bmatrix} \in \mathfrak{g}$$
$$\text{and} \quad (\omega, v) \in \mathbb{R}^3 \circledS \mathbb{R}^3 .$$

Physically, ξ represents the linear $v = [v_x, v_y, v_z]^T$ and angular $\omega = [\omega_x, \omega_y, \omega_z]^T$ velocities relative to the instantaneous body-frame. Similarly, for $\mathcal{G} = \mathrm{SE}(2)$ and $\mathfrak{g} = \mathrm{se}(2)$, we have $\omega \in \mathbb{R}$, $v = [v_x, v_y]^T \in \mathbb{R}^2$, and

$$\xi = g^{-1}\dot{g} = \begin{bmatrix} 0 & -\omega & v_x \\ \omega & 0 & v_y \\ 0 & 0 & 0 \end{bmatrix} \in \mathfrak{g}\,, \text{ and } \ (\omega, v) \in \mathbb{R} \circledS \mathbb{R}^2 .$$

3.2 Landmark Kinematics

Consider the group action of an element $g \in \mathcal{G}$ that translates a point $p_b = [x_b, y_b, z_b, 1]^T \in \mathbb{E}^3$ in the robot based coordinate system to the fixed world frame $p_w = [x_w, y_w, z_w, 1]^T$, via

$$p_w = g\, p_b. \tag{5}$$

Since the velocity of any fixed point in the world frame is zero, then its velocity in robot body based frame can be obtained by differentiating (5), i.e.,

$$\dot{p}_b = -g^{-1}\dot{g}\, p_b = -\xi\, p_b\,. \tag{6}$$

Consider the trivial "landmark function" $\ell : \mathcal{G} \to \mathcal{L}$, where $L = \mathbb{E}^n$ represents a single feature point and $\mathcal{G} = \mathrm{SE(n)}$, $n = 2$ or $n = 3$. Then

$$\ell(g) = g^{-1}\, p_w = p_b\,. \tag{7}$$

By using the above tangent space identification, the tangent map $T\ell : T\mathcal{G} \to T\mathcal{L}$ admits a convenient matrix representation, J_ℓ, given by

$$\dot{p}_b = \overbrace{\begin{bmatrix} \hat{p}_b & -I_{3\times 3} \\ 0^T & 0^T \end{bmatrix}}^{J_\ell} \begin{bmatrix} \omega \\ v \end{bmatrix}, \qquad \text{where} \quad \hat{p}_b = \begin{bmatrix} 0 & -z_b & y_b \\ z_b & 0 & -x_b \\ -y_b & x_b & 0 \end{bmatrix}. \tag{8}$$

Again, for SE(2) we have $\omega \in \mathbb{R}$, $v = [v_x, v_y]^T \in \mathbb{R}^2$, $p_b = [x_b, y_b, 1]^T, p_w = [x_w, y_w, 1]^T \in \mathbb{E}^2$, and

$$J_\ell = \begin{bmatrix} \hat{p}_b & -I_{2\times 2} \\ 0 & 0^T \end{bmatrix}, \quad \text{where} \quad \hat{p}_b = \begin{bmatrix} -y_b \\ x_b \end{bmatrix}. \tag{9}$$

It is straight forward to generalize the above expressions for landmark functions ℓ that incorporate multiple landmark features.

3.3 Feature Kinematics

Suppose $\mathcal{L} \subset \mathbb{E}^n$ is some set of landmarks, that is, points in the world, fixed in a world frame, and $\mathcal{S}$ is the sensor feature space. Let $\ell : \mathcal{G} \to \mathcal{L}$ denote the mapping from robot configuration to relative landmark configuration, as described above. Let $h : \mathcal{L} \to \mathcal{S}$ be the sensorial mapping. Then $Th : T\mathcal{L} \to T\mathcal{S}$ is the tangent map (or Jacobian) relating landmark velocities to feature velocities, with matrix representation J_h, namely

$$\dot{s} = J_h \dot{p}. \tag{10}$$

where $s = h(p)$ denotes the sensor measurement.

The Jacobian for our simple "sonar + vision" sensorium defined in the previous section can be found by differentiating (4), namely

$$\dot{s} = \begin{bmatrix} \frac{\dot{y}}{x}\lambda - \frac{y\dot{x}}{x^2}\lambda \\ (y^2+x^2)^{-\frac{1}{2}}(y\dot{y}+x\dot{x}) \end{bmatrix}$$

or

$$\dot{s} = J_h \dot{p} \tag{11}$$

where

$$J_h = \begin{bmatrix} \frac{\eta}{\delta} & -\frac{\gamma\eta}{\lambda\delta} & 0 \\ \frac{\gamma}{\eta} & \frac{\lambda}{\eta} & 0 \end{bmatrix}$$

is the sensor Jacobian obtained by noticing

$$p = \begin{bmatrix} x \\ y \\ 1 \end{bmatrix} = h^{-1}(s) = \begin{bmatrix} \frac{\delta\lambda}{\eta} \\ \frac{\delta\gamma}{\eta} \\ 1 \end{bmatrix} \tag{12}$$

where $\eta = (\gamma^2 + \lambda^2)^{\frac{1}{2}}$.

3.4 Extended Visual Servoing

The control objective is to move a robot to align the sensor measurements, $s = h \circ \ell(g)$, with a predefined value s^*. If we define $\mathcal{U}$ as the control input space of the robot and $\mathcal{G}$ its configuration state space, then the control input $u \in \mathcal{U}$ of a mobile robot will change the pose (position and orientation) $g \in \mathcal{G}$ of the robot through robot kinematics and dynamics, which in turn will update the location of landmarks $\mathcal{L}$ with respect to the robot frame. Then the on board sensors will further map the landmarks to sensor space $s \in \mathcal{S}$.

For the present work, we posit a purely kinematic plant model, actuated in the body frame. For fully actuated systems, $\dim \mathcal{U} = \dim \mathfrak{g}$, but we do not limit ourselves to that case. In fact, the example investigated in Sec. 4 has fewer control degrees of freedom than rigid body degrees of freedom. Let M be the mapping between control input and body velocity. Then the following commutative diagram describes the flow of velocities

$$\begin{array}{ccccccc} \mathcal{U} & \xrightarrow{M} & T\mathcal{G} & \xrightarrow{T\ell} & T\mathcal{L} & \xrightarrow{Th} & T\mathcal{S} \\ & & \downarrow & & \downarrow & & \downarrow \\ & & \mathcal{G} & \xrightarrow{\ell} & \mathcal{L} & \xrightarrow{h} & \mathcal{S} \end{array}$$

or, in coordinates

$$\dot{s} = \overbrace{J_h\, J_\ell\, M}^{J}\; u\,.$$

There are now many possible control inputs. Suppose that $\dot{s}^*$ is a desired velocity in sensor space. Then, we could let

$$u = J^\dagger \dot{s}^* \tag{13}$$

where $J^\dagger$ is the pseudo-inverses of J. In some cases, it may actually be possible to find an exact inverse to J. For example, if the spaces $\mathcal{G} \simeq \mathcal{L} \simeq \mathcal{S}$ are diffeomorphic, and ℓ and h are diffeomorphisms, and the system is fully actuated, so that M is nonsingular, then we can compute J^{-1}, as we have done for visual servoing in several prior contexts contexts [4, 5, 15]. In this report, we consider a case in which J is full rank, even though $\mathcal{G}$ and $\mathcal{L}$ are not diffeomorphic.

4 Example: Rolling Penny Robot

Consider a cart-like "rolling penny" or "Hilare" robot. The configuration of the robot and its equivalent rolling penny illustration are shown in Fig. 3. A camera is fixed to the robot body such that its coordinate system is identical to the body frame, and its optical axis is aligned with the X-axis of the robot. In addition, there is a sonar ring with origin also coincident with the body frame origin.

For illustration purposes, we assume that there is only one object in the field of view of the robot, and that the camera observes a single feature of the object; for example one could use the image-plane center of mass as done in [4, 15], to obtain the overall direction of the center of mass of the object relative to the robot. We consider convex objects, toward the robot, such that the reflecting point of the object is coincident with the center

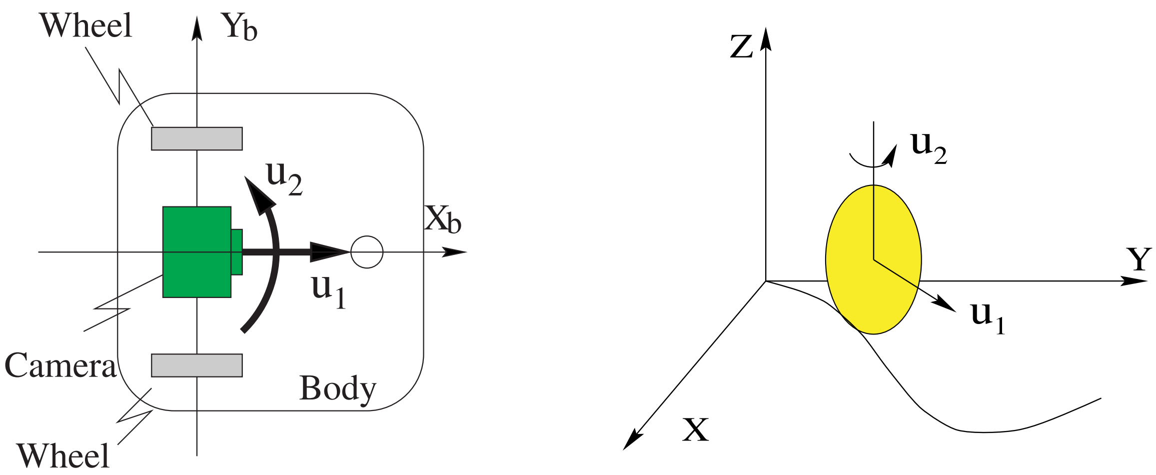

Figure 3: Top view of the configuration of a cart-like robot (left). The equivalent rolling penny model (right).

of the color mass as illustrated in Fig. 4. However, we believe this restriction may be relaxed or modified to accommodate a different selections of image features.

For simplicity, as mentioned, the sonar and camera are configured in a way such that the center of the sonar ring is the origin of the camera frame. Thus, the coordinate systems for the camera, sonar and robot are identical. Further, although the sonar sensors are always installed as a ring and theoretically could obtain a 180° or 360° field of view, we restrict ourselves to the portion that coincident with the field of view of the camera.

Recall the mappings s and ℓ for our "camera + sonar" sensorium, measuring a single point, are given by (4) and (7), summarized for convenience here:

$$p = \begin{bmatrix} x \\ y \\ 1 \end{bmatrix} = \ell(g) := g^{-1}\, p_w\,,$$

$$s = \begin{bmatrix} \gamma \\ \delta \end{bmatrix} = h(p) := \begin{bmatrix} \frac{y}{x}\lambda \\ (x^2+y^2)^{\frac{1}{2}} \end{bmatrix}\,,$$

where $g \in \mathcal{G} = \mathrm{SE}(2)$, $p \in \mathcal{L} = \mathbb{E}^2$ and $s \in \mathcal{S} = \mathbb{R} \times \mathbb{R}^+$. Thus, $s = h \circ \ell(g)$.

The two inputs of the robot are the forward speed u_1 and the angular velocity u_2, thus

$$\begin{bmatrix} \omega \\ v \end{bmatrix} = \overbrace{\begin{bmatrix} 0 & 1 \\ 1 & 0 \\ 0 & 0 \end{bmatrix}}^{M} u$$

Recall that $\dot{s} = J_h\, J_\ell\, M u$ where J_h is given by (11) and J_ℓ is given by (8). Thus we have

$$\dot{s} = J u \tag{14}$$

where

$$J = J_h\, J_\ell\, M = \begin{bmatrix} \frac{\gamma\eta}{\delta\lambda} & -\frac{\eta^2}{\lambda} \\ -\frac{\lambda}{\eta} & 0 \end{bmatrix}\,.$$

Note that $\dim \mathcal{G} > \dim \mathcal{S}$. However, we have chosen $\dim \mathcal{S} = \dim \mathcal{U} = 2$. Thus, noting that $\eta^2 = \lambda^2 + \gamma^2 > 0$, the inverse

$$J^{-1} = \begin{bmatrix} 0 & -\frac{\eta}{\lambda} \\ \frac{\lambda^2}{\eta} & \frac{\eta\gamma}{\delta} \end{bmatrix}$$

is well defined for $\delta > 0$. Given desired features $s^* = [\gamma^*,\ \delta^*]^T$, we can apply a simple proportional control law with positive definite gain matrix K, namely

$$u = J^{-1} K (s^* - s) \tag{15}$$

which implies

$$\dot{\tilde{s}} = -K\tilde{s} \tag{16}$$

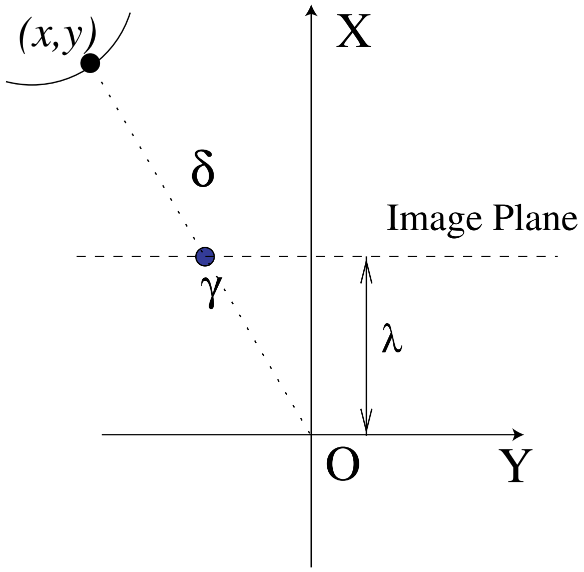

Figure 4: Top view of a planar mobile robot with both camera and sonar.

where $\widetilde{s} = (s - s^*)$ is the sensorial error.

To avoid collisions with the feature object, and to keep the feature within the field-of-view, one could easily introduce a Navigation Function, as done in [5]. In this case it is straight forward since the space $\mathcal{S} = \mathbb{R} \times \mathbb{R}^+$ is so simple.

5 Simulation Experiments

For our simulation experiments, a target resides at $p_w = [6, 3]^T$m in the world frame. The initial location of the robot body frame was coincident with the world frame at $t = 0$. As described, we assume for convenience that the coordinate frames of the sonar ring and camera coincide with the body frame. Since the camera is assumed calibrated, we scale the image measurement to achieve an effective focal length of $\lambda = 1$m.

Let $s^* = [0, 2]^T$m, a goal that corresponds to moving the mobile such that the object is right in front of the robot, $\gamma^* = 0$, at a distance of $\delta^* = 2m$. Then applying the approach above, we can easily obtain closed loop control for the task with a given tolerance (that will depend in practice on the true pixel resolution of the camera, and the sonar resolution).

In Fig. 5, the subplot "Control Inputs" shows the input translational and rotational velocities of the robot with time. The subplot "Image Feature" is scaled to pixel coordinates, assuming a true focal length of 5mm, and 120pixels/mm. The "Distance" subplot illustrates the change of γ, the horizontal position of the object in the image plane (corresponding to the sonar measurement).

In Fig. 6, the subplot "Body" shows the trajectory of the target observed by the robot in the robot body frame. The subplot "Global" shows the trajectory of the mobile robot in the global frame during the process of moving and turning to approach the target with the desired distance and orientation.

As shown by this anecdotal simulation, the system converges as expected. Notice that since we are only controlling 2DOF, there is a one dimensional symmetry that we do not control – it corresponds to a circle around the target for which the robot is facing inward. If the target were moving in time, the algorithm could be modified for tracking, as done in [3].

6 Summary

This work builds on and enhances many techniques developed for visual servoing. For example, one can still apply Navigation Function to avoid obstacles and keep features in the field-of-view [6], or integrate motion planning to achieve long distance movement and obstacle avoidance [16]. By applying extended visual servoing, we can take advantage of mathematical framework of visual servoing, without limiting ourselves to a single sensor modality. There are several advantages to this approach.

First, using sensor features from multiple sensors, we can obtain a Jacobian with increased rank, hence map the feature velocity to a larger subset of the robot's motion. With a bit of ingenuity, it may in some cases be possible to find a diffeomorphism between the robot's motion and the sensorial feature motion. In the case of an underactuated robot, like the example we studied, we described an extended feature constellation that allowed us to use feedback linearization on a subset of the available configurations, giving rise to a one-dimensional set of solutions.

A second advantage arises by selecting sensors that complement each other. Even in cases where there is a known diffeomorphism between sensor and robot co-

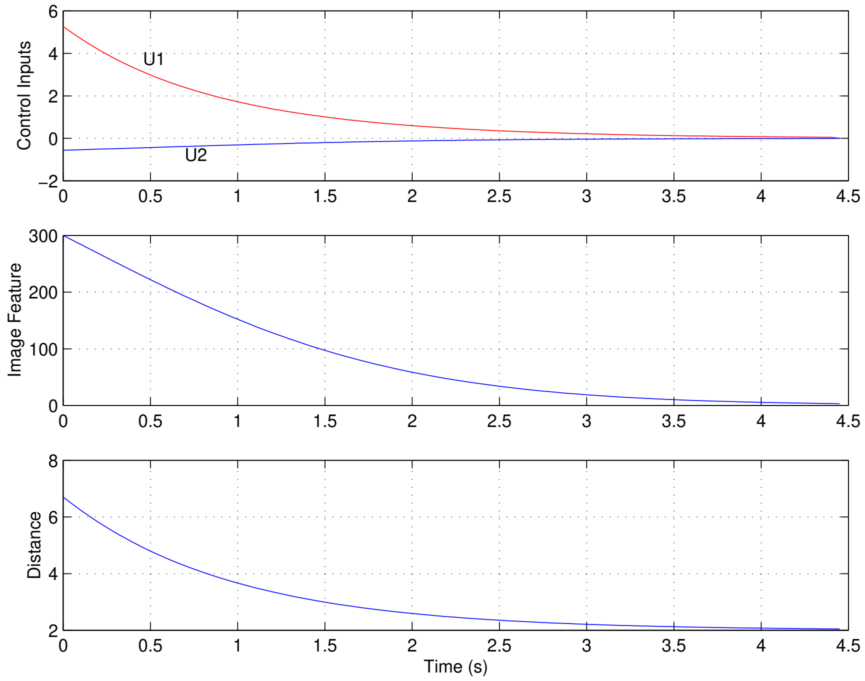

Figure 5: Control inputs and controlled sensor features.

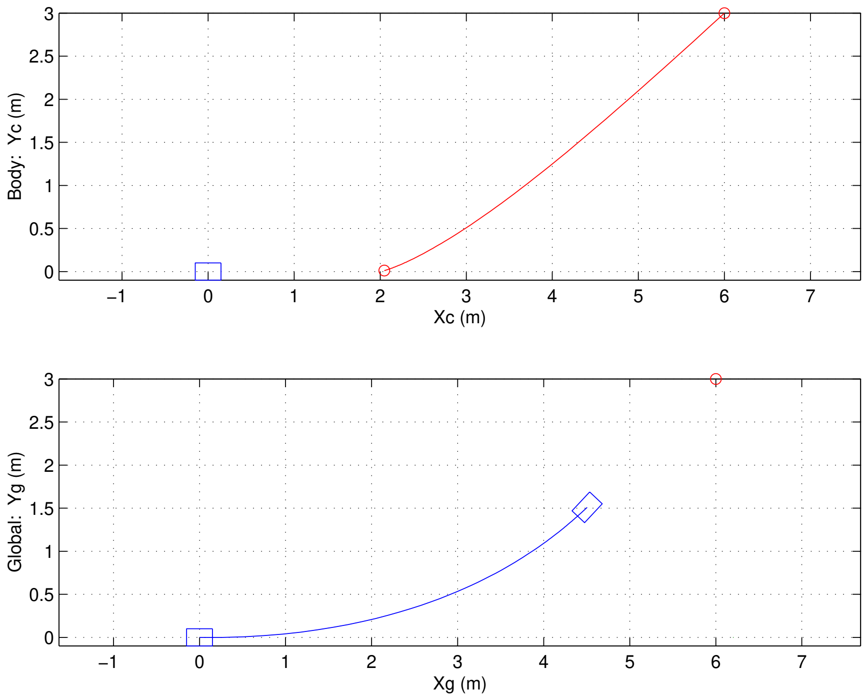

Figure 6: Target trajectory in body frame and robot trajectory in global frame.

ordinates, representing the Jacobian may be "messy" in image coordinates [5], or may require special targets [4, 16]. However, the sensor Jacobian in the present paper may be compactly written making very few assumptions about target geometry.

Third, as we noticed in, Section 2 and 3, although the landmarks can be expressed in a global frame, the expressions are not used in derivation of extended visual servoing. Hence, the algorithm is insensitive to the geometric model of the landmarks. Admittedly the landmark feature set was trivial in the present context, and so more must be done to see how these ideas can be generalized.

Fourth, by integrating the sensor features in the body based coordinate system, we can bypass the common difficulties of sensor fusion, e.g. the extra step of transferring the feature information back to the global frame, and then calculating the control input in the global coordinate system, which has to be remapped into the robot frame.

Finally, although we derived the extended visual servoing control algorithm based on a kinematically actuated planar mobile robot, we believe that extending it to both dynamically actuated mobile robots such as a submarine or a blimp, or employing the algorithms for a the fixed-camera and moving robot arm should be possible.

Acknowledgments

The second author was supported by DARPA/ONR under grants N00014-98-1-0747 and N66001-00-C8026, and NSF under grant ECS-9873474.

References

[1] R. Bajcsy, G. Kamberova, R. Mandelbaum, and M. Mintz. Robust fusion of position data. In *Workshop on Foundations of Information/Decision Fusion*, pages 1–7, Washington, D.C. USA, August 1996.

[2] Hakyoung Chung, Lauro Ojeda, and Johann Borenstein. Sensor fusion for mobile robot dead-reckoning with a precision-calibrated fiber optic gyroscope. In *IEEE International Conference on Robotics and Automation*, pages 3588–3593, Seoul, Korea, May 21-26 2001.

[3] Noah Cowan, Omid Shakernia, Rene Vidal, and Shankar Sastry. Vision-based follow the leader. In *Intelligent Robots and Systems*, Las Vegas, NV, October 2003. IEEE. submitted.

[4] Noah J. Cowan and Dong Eui Chang. *Second Workshop on Control Problems in Robotics and Automation*, chapter Toward Geometric Visual Servoing. Springer-Verlag, 2002.

[5] Noah J. Cowan, Joel D. Weingarten, and Daniel E. Koditschek. Visual servoing via navigation functions. *Transactions on Robotics and Automation*, 18(4), August 2002.

[6] Noah J. Cowan, Joel D. Weingarten, and Daniel E. Koditschek. Visual servoing via navigation functions. *IEEE Transactions on Automatic Control*, 18:4, August 2002.

[7] Bernard Espiau, Francois Chaumette, and Patrick Rives. A new approach to visual servoing in robotics. *IEEE Transactions on Robotics and Automation*, 8(3):313–326, June 1992.

[8] Seth Hutchinson, Gregory D. Hager, and Peter I. Corke. A tutorial on visual servo control. *IEEE Transactions on Robotics and Automation*, 12(5):651–670, 1996.

[9] B. Lamiroy, B. Espiau, N. Andreff, and R. Horaud. Controlling robots with two cameras: How to do it properly. In *IEEE International Conference of Robotics and Automation*, pages 2100–2105, San Francisco, California, May 2000.

[10] E. Malis, F. Chaumette, and S. Boudet. 2 1/2 d visual servoing. *IEEE Transactions on Robotics and Automation*, 15(2):238–250, April 1999.

[11] Robert Mandelbaum. *Sensor Processing for Mobile Robot Localization, Exploration and Navigation.* PhD thesis, University of Pennsylvania, Philadelphia,PA, October 1995.

[12] Jerrold E. Marsden and Tudor S. Ratiu. *Introduction to Mechanics and Symmetry.* Springer, 2 edition, 1999.

[13] William J. Wilson, Carol C. Williams Hulls, and Graham S. Bell. Relative end-effector control using Cartesian position based visual servoing.

IEEE Transactions on Robotics and Automation, 12(5):684–696, 1996.

[14] Teruko Yata, Akihisa Ohya, and Shin'ichi Yuta. A fast and accurate sonar-ring sensor for a mobile robot. In *International Conference on Robotics and Automation*, pages 630–636, 1999.

[15] Hong Zhang and James P. Ostrowski. Visual servoing with dynamics: Control of an unmanned blimp. In *International Conference on Robotics and Automation*, pages 618–623, May 1999.

[16] Hong Zhang and James P. Ostrowski. Visual motion planning for mobile robots. *IEEE Transactions on Robotics and Automation*, 18:2:199–208, April 2002.